Title: Successive range expansion promotes diversity and accelerates evolution in spatially structured microbial populations

Authors: Felix Goldschmidt[1, 2], Roland R. Regoes[1], David R. Johnson[2]

Affiliations: [1]Department of Environmental Systems Science, ETH Zürich, 8092 Zürich, Switzerland, and [2]Department of Environmental Microbiology, Eawag, 8600 Dübendorf, Switzerland

Corresponding author address: David R. Johnson, Department of Environmental Microbiology, Eawag, Überlandstrasse 133, 8600 Dübendorf, Switzerland. Phone: +41 58 765 5520. Fax: +41 58 765 5802. Email, david.johnson@eawag.ch

Running title: Successive range expansion promotes diversity

Subject category: Microbial population and community ecology

Keywords: Range expansion, spatial diversity, microbial ecology, microbial interactions, cross-feeding, landscape ecology

This document is the accepted manuscript version of the following article:
Goldschmidt, F., Regoes, R. R., & Johnson, D. R. (2017). Successive range expansion promotes diversity and accelerates evolution in spatially structured microbial populations. ISME Journal, 11(9), 2112-2123. https://doi.org/10.1038/ismej.2017.76

Abstract

Successive range expansions occur within all domains of life, where one population expands first (primary expansion) and one or more secondary populations then follow (secondary expansion). In general, genetic drift reduces diversity during range expansion. However, it is not known whether the same effect applies during successive range expansion, mainly because the secondary population must expand into space occupied by the primary population. Here we used an experimental microbial model system to show that, in contrast to primary range expansion, successive range expansion promotes local population diversity. Because of spatial constraints imposed by the presence of the primary population, the secondary population forms fractal-like dendritic structures. This divides the advancing secondary population into many small sub-populations and increases intermixing between the primary and secondary populations. We further developed a mathematical model to simulate the formation of dendritic structures in the secondary population during succession. By introducing mutations in the primary or dendritic secondary populations, we found that mutations are more likely to accumulate in the dendritic secondary populations. Our results thus show that successive range expansion can increase intermixing over the short term and genetic diversity over the long term. Our results therefore have important implications for predicting the ecological processes and evolutionary fates of microbial communities.

Introduction

Range expansion is a universal process that affects the life histories of nearly every microbial community (Tilman and Kareiva, 1997). Range expansion occurs when one or more populations expand into previously unoccupied space. Previous theoretical studies and experiments with synthetic microbial communities demonstrated that range expansion can dramatically reduce intermixing between populations and deteriorate local population diversity (Hallatschek *et al*., 2007; Excoffier *et al*., 2009) (Figure 1a). An important feature of these experiments is that they have largely investigated scenarios where different microbial populations expand into unoccupied space simultaneously, which occurs when their growth properties are nearly identical. While there are some situations in nature where this may occur, *e.g*. following the retraction of glaciers after an ice-age (Hewitt, 2000), these situations are not likely the typical case. Instead, some populations likely expand first (referred to as the primary expansion or primary population) while other populations follow afterwards (referred to as the secondary expansion or secondary population). This process is known as succession and is pervasive in nature (Connell and Slatyer, 1977). For example, after a forest fire, grasses expand before trees. A key point is that because the primary population expands first, it changes the environment. The secondary population must therefore expand and establish within a landscape that is already modified by the primary population, which might constrain and affect their potential expansion (Connell and Slatyer, 1977).

While successive range expansions have primarily been studied for vegetative communities, such as the forest fire example described above, they likely occur for all organisms. For example, there is evidence for two major expansions of humans in the Paleolithic. The first

63 expansion presumably consisted of hunters and gatherers that moved out of Africa. The
64 second expansion consisted of farmers that expanded from the Middle East into areas that
65 were already colonized by the hunters and gatherers (Sokal *et al*., 1991; Cacalli-Sforza *et al*.,
66 1993). Succession may also occur among the smallest of organisms: microbes. Microbial
67 biofilms on teeth are often periodically removed via brushing. Thereafter, primary
68 populations attach to the surfaces of cleaned teeth via specialized surface proteins and
69 begin to expand. Secondary populations then attach to those biofilms and expand through
70 the biofilms produced by the primary populations (Rickard *et al*., 2003; Kolenbrander *et al*.,
71 2010).
72
73 Although successive expansions are likely pervasive in natural microbial ecosystems, they
74 have not been widely studied experimentally or theoretically. Conceptually, succession can
75 be seen as two temporally segregated expansions of microorganisms (Figure 1b), which
76 implies a complete segregation of the two populations in the direction of the expansion. The
77 consequence is a reduction of intermixing of the two populations, and thus a reduction of
78 local population diversity, which may have important consequences on microbial processes.
79
80 The objective of this study was to quantitatively assess how successive expansion affects
81 local population diversity (intermixing) between primary and secondary populations. We
82 expect successive expansion to reduce intermixing between populations and, consequently,
83 reduce local population diversity. To address this objective, we constructed an experimental
84 system that allowed us to impose a metabolic interaction that promotes successive
85 expansion of two populations of the bacterium *Pseudomonas stutzeri*. *P. stutzeri* is a
86 facultative anaerobe that can use nitrate as an electron acceptor in the absence of oxygen in

a process called denitrification (Lalucat *et al*., 2006). *P. stutzeri* can perform the complete denitrification pathway (referred to as the complete degrader), in which nitrate is sequentially reduced to nitrite, nitric oxide, nitrous oxide, and finally to dinitrogen gas (Zumft, 1997). We previously deleted specific genes within the *P. stutzeri* genome to construct two isogenic mutant strains that cross-feed the metabolic intermediate nitrite (Lilja and Johnson, 2016). One strain partially metabolizes nitrate to nitrite (referred to as the producer) and the other strain metabolizes nitrite to dinitrogen gas (referred to as the consumer). Because the consumer cannot grow before the producer when nitrate is provided as the growth-limiting substrate, we expected the cross-feeding populations to undergo successive range expansion when grown together in the absence of oxygen, where the producer expands first and the consumer follows afterwards. Each population carries a gene encoding for a different fluorescent protein, thus allowing us to quantify the resulting spatial patterns and the magnitude of intermixing between populations using image analysis. We then compared the results for co-cultures of the producer and consumer (*i.e*., two strains that cross-feed nitrite and presumably expand sequentially) with the results for co-cultures of two complete degraders (*i.e*., two ancestral strains that completely reduce nitrate to dinitrogen gas, have the same growth properties and therefore expand simultaneously). In addition, we developed a two-dimensional reaction-diffusion model that allowed us to predict the long-term effects of successive range expansion on local genetic diversity within the primary or secondary expansion.

Methods

Bacterial strains and growth conditions. We used a previously developed experimental microbial system for all our experiments, which is described in detail elsewhere (Lilja and Johnson, 2016). In short, the *narG, nirS,* and *comA* genes were deleted from *P. stutzeri* A1501. The producer contains a deletion in *nirS* gene, which encodes for the reduction of nitrite to nitrous oxide, and can only convert nitrate to nitrite (Zumft, 1997). The consumer contains a deletion in *narG*, which encodes the enzymes for the degradation of nitrate to nitrite, and can only convert nitrite to dinitrogen gas (Zumft, 1997). *comA*, which is a transporter required for competence, was deleted to prevent recombination during experimentation. To enable fluorescence microscopy, we introduced different fluorescent protein-encoding genes (green- or cyan-fluorescent protein-encoding genes) into the strains as described in the Supplementary Information.

Anaerobic colony expansion assay. We implemented a modified anaerobic version of the expansion experiment described by Hallatscheck *et al*. (2007). First, we grew different strains of *P. stutzeri* separately overnight in LB medium under aerobic conditions. We then adjusted the cell densities of the cultures (see the Supplementary Information for details), mixed the cultures according to experimental needs as described in the results section (*e.g*. the producer and consumer at a ratio of 1:1 [cell number:cell number]) and transferred the cultures to an anaerobic glove box. We then inoculated 2-□l drops of the mixtures onto the middles of anaerobic agar plates (one drop per plate), allowed the drops to dry for 1h, and incubated the plates at 21°C for up to 4 weeks. We finally exposed the plates for 1 hour to ambient air to induce maturation of the fluorescent proteins and took images with a confocal microscope (Leica TCS SP5 II). We performed image analysis in FIJI and data analysis in R (complete descriptions are available in the Supplementary Information).

Intermixing index. We defined intermixing similar to the definitions described previously (Pielou, 1966; Momeni *et al*., 2013). Briefly, we devided the measured number of intersections between different populations at a given radius (N_r) by the expected number of intersections for a random spatial distribution of two populations ($E(N_r)$) (a complete description is available in the Supplementary Information). We thus defined intermixing at a given radius (I_r) as:

$$I_r = \frac{N_r}{E(N_r)} = \frac{N_r}{\pi r/2} \quad (1)$$

Modeling. We developed a spatially explicit reaction-diffusion model to simulate successive expansion of two populations that exchange a metabolic intermediate. The model consists of a producer (P), a consumer (C), and two substrates nitrate (N_1) and nitrite (N_2), each of which is modeled on a separate square lattice of size 1024x1024. Initially, only substrate N_1 is present while substrate N_2 is produced by P. At the beginning of the simulations, P and C are randomly inoculated in a circular area in the middle of the grid and can then expand. To efficiently model the two populations and two substrates on large spatial grids, a part of the code was parallelized using GPU acceleration as described elsewhere (van de Koppel *et al*., 2011). The model is written in CUDA, which allows the execution of parts of the code on a graphics processor. We analyzed and visualized the model output in Matlab.

The equations for the bacteria consist of a diffusion term and a growth term. The diffusion terms of the producer and consumer are not constant, but instead depend on the local concentrations of the substrates, the densities of the two strains, and a local anisotropy term Ω. Diffusion of the cells is only possible as long as the respective substrate is present.

Moreover, diffusion is facilitated by the focal local population density (Mimura *et al*., 2000) and hindered by the local population density of the other population (note how P and C are swapped in equations 2b and 3b). Ω is a locally varying random number with values of either 0 or 100 that is assigned to each grid cell. The values and distribution of Ω can be used to change the properties of the dendritic pattern. □ is a scaling factor to balance the expansion speed between the two populations. Growth is modeled with a Monod-type term with maximal growth rates ($r_{p,c}$) and substrate specific half-velocity constants ($K_{1,2}$).

$$\frac{\partial P}{\partial t} = \sigma\nabla\left(D_p\nabla \mathrm{P}\right) + r_p P\frac{N_1}{K_1+N_1} \quad (2a)$$

$$D_p = \frac{N_1(1+P)}{1+\Omega C} \quad (2b)$$

$$\frac{\partial C}{\partial t} = \nabla(D_c\nabla \mathrm{C}) + r_c C\frac{N_2}{K_2+N_2} \quad (3a)$$

$$D_c = \frac{N_2(1+C)}{1+\Omega P} \quad (3b)$$

The equations of the two substrates consist of a constant diffusion term (with diffusion constants D_{N1} and D_{N2}), a consumption term that is proportional ($\nu_{1,2}$) to the growth of the respective bacterial populations and for N_2 a production term that is equal to the consumption of N_1, reflecting the 1:1 stoichiometric relationship of the production of nitrite from nitrate.

$$\frac{\partial N_1}{\partial t} = D_{N1}\nabla^2 N_1 - \nu_1 r_p P\frac{N_1}{K_1+N_1} \quad (4)$$

$$\frac{\partial N_2}{\partial t} = D_{N2}\nabla^2 N_2 + \nu_1 r_p P\frac{N_1}{K_1+N_1} - \nu_2 r_c C\frac{N_2}{K_2+N_2} \quad (5)$$

182

183 We used generic parameters for all simulations (parameters are provided in Supplementary
184 Table 3).

185

186

187 **Results**

188

189 **Dendrite formation increases intermixing.** We grew co-cultures of two complete degraders
190 (simultaneous expansion) or co-cultures of the producer and the consumer (successive
191 expansion) on anaerobic agar plates supplied with nitrate as the growth-limiting substrate.
192 The complete degraders formed sectors with saw-tooth like boundaries between the two
193 populations. These boundaries were oriented parallel to the axis of expansion, similar to the
194 patterns described previously for the expansion of metabolically identical populations of *E.*
195 *coli* (Hallatschek *et al*., 2007) (Figure 2a). In contrast, the producer and consumer expanded
196 successively; the producer expanded first while the consumer followed (Figure 2b). The
197 producer completely covered the expansion area and had a relatively continuous expansion
198 front similar to that observed for the complete degraders. In contrast, the consumer
199 unexpectedly formed branched dendrites that extended into the space occupied by the
200 producer (Figure 2b). Each dendrite typically originated at a single point from the inoculation
201 zone (referred to as a stem) and branched during expansion (referred to as tips). The tips
202 were directly connected to a single stem and had clear boundaries with the producer. The
203 dendrites typically did not touch each other, but were instead separated by a thin layer of
204 the producer. The number of dendrites decreased with the direction of the expansion,

qualitatively similar to the decrease in the number of sectors between completely degrading strains (Hallatschek *et al*., 2007).

The dendritic nature of the secondary expansion caused increased intermixing of the two populations, which was opposite to our initial expectation (Figure 1). To quantify this, we defined an intermixing index similar to previous studies (Pielou, 1966; Momeni *et al*., 2013) as the number of transitions between the consumer and producer divided by the expected number of transitions from a random distribution at a certain circumference (see the Supplementary Information for a complete description). An intermixing index higher than one indicates more mixing than a random distribution while an intermixing index lower than one indicates more segregation than a random distribution. Note that in natural systems the latter is the predominant case (Pielou, 1966). We found that intermixing was relatively constant in the inoculation zone (mean = 0.1609, SE = 0.0004), but increased in the secondary expansion (mean = 0.1743, SE = 0.0005) (Figure 2c). Overall intermixing increased by 8.35% during secondary expansion (Mann-Whitney test, $p < 2.2e\text{-}16$). Our results thus show that branching of the secondary expansion increased intermixing, which is fundamentally different from the demixing effect of drift during primary expansion (Hallatschek *et al*., 2007).

Spatial constraints cause dendrite formation. To infer the mechanism of branching during succession, we analyzed the structure of the dendritic pattern in more detail. The dendrites formed by the consumer qualitatively resemble the fractal branching-type patterns generated by the diffusion-limited aggregation (DLA) process. DLA is a computer model to generate dendritic patterns that have fractal properties, meaning that the dendritic pattern

repeats itself over several orders of magnitude of observation. Since its discovery, DLA has received increasing attention because similar patterns have been repeatedly observed in diverse natural systems, including bacterial growth on agar plates (Fujikawa and Matsushita, 1989). The fractal properties are quantified by the fractal dimension, which can be measured using image analysis. We found that the fractal dimension of the consumer dendrites (mean D=1.73, standard deviation (SD)=0.03, N=8) is compatible with the fractal dimension of the DLA process (1.71) (May and Maher, 1989).

The mechanisms causing the formation of DLA-type dendrites in bacteria have typically been attributed to diffusion limitation of the growth substrate or spatial constraints, such as agar hardness (Ben-Jacob *et al*., 1994; Mimura *et al*., 2000). Our observed similarity of pattern formation during expansion of the consumer with DLA fractals thus suggests that one or both of these two mechanisms could have caused the formation of the observed dendrites. The first is that the expansion of the consumer is constrained by the availability of the growth-limiting cross-fed substrate nitrite. The second is that the expansion of the consumer is spatially constrained and must advance via mechanical cell shoving through the producer (Mather *et al*., 2010). Both mechanisms can produce patterns with the same fractal dimension as DLA and can therefore not be distinguished by simple observation of the pattern (Mathiesen *et al*., 2006). We therefore designed experiments to analyze the relative contributions of the two mechanisms to dendrite formation during the expansion of the consumer.

To test whether substrate limitation caused the formation of dendrites, we grew co-cultures of the producer and consumer on agar plates containing exogenous and excess supplies of

253 both nitrate and nitrite, thus reducing the possibility that the limited amount of nitrite
254 formed via cross-feeding caused the dendrite formation during expansion of the consumer.
255 We found that, even when both nitrate and nitrite were provided exogenously, the two
256 populations continued to form two successive wave fronts and the consumer still expanded
257 after the producer. More importantly, even though the consumer had greater availability of
258 its growth-limiting substrate nitrite than the producer (note that nitrite was provided
259 exogenously and produced via the activity of the producer), it nevertheless still produced
260 dendritic patterns during expansion that were qualitatively similar to those observed when
261 only nitrate was provided exogenously (Figure 3a).
262
263 To further exclude the possibility that the consumer is limited by the availability of nitrite,
264 we grew two differently labeled consumers (*i.e*. they produced either green or red
265 fluorescent protein) together on agar plates containing nitrite as the only available electron
266 acceptor. The consumer did not form dendrites when growing in the absence of the
267 producer. Similar to the completely degrading strains, the consumers formed sectors with
268 boundaries that lied approximately parallel to the direction of expansion (Figure 3b). These
269 results together indicate that substrate availability was not the main growth-limiting factor,
270 and therefore not the main cause of dendrite formation.
271
272 This leaves the hypothesis that dendrite formation during expansion of the consumer was
273 mainly caused by spatial constraints imposed on the consumer by having to expand into
274 space previously occupied by the producer. If this were a general mechanism, one would
275 expect that different strains that grow into previously occupied space produce similar
276 patterning. To test this hypothesis, we devised an experiment where the producer had to

277 expand into space occupied by the consumer (note that this is the reverse of the expansion
278 ordering imposed previously). To accomplish this, we inoculated the producer at low
279 frequencies (below 100 cells per colony) on plates containing exogenous supplies of both
280 nitrate and nitrite. The producer population thus consisted of isolated cells that were
281 embedded within the consumer biofilm and had to grow through the consumer to expand.
282 We found that the producer also formed dendrites when expanding into space occupied by
283 the consumer (Figure 3c), indicating that spatial constraints were indeed an important
284 process causing dendrite formation in the secondary expansion.
285
286 **Mutants establish more readily in the secondary expansion.** The fundamentally different
287 shape of the dendritic secondary expansion raises the question of whether the different
288 shapes of the non-dendritic primary and dendritic secondary expansions cause differences in
289 the long-term molecular evolution of the populations. The idea here is that a mutant that
290 occurs during expansion has to compete with the surrounding actively growing ancestral
291 population (for space and/or nutrients). The larger this active population is, the harder it is
292 for the mutant to establish and increase in frequency (Excoffier *et al.*, 2009). In the
293 continuous non-dendritic primary expansion, the active population is relatively large, making
294 it harder for the mutant to establish. In contrast, in the dendritic secondary expansion, the
295 active population at the tip of an expanding dendrite is very small, making it easier for the
296 mutant to establish (Excoffier and Ray, 2008). The long-term effect would therefore be a
297 higher accumulation of mutations in a dendritic secondary expansion than in a non-dendritic
298 primary expansion.
299

We developed a mathematical model that allowed us to study the dynamics of successive range expansions and the branching of the dendritic secondary expansion on evolution. Following earlier approaches of modeling dendritic microbial expansion on agar plates (Golding *et al*., 1998; Mimura *et al*., 2000), we chose a reaction-diffusion model with non-linear diffusion terms for the microbial populations. The model consists of lattices for the two populations (producer and consumer) and the two corresponding growth-limiting substrates (nitrate and nitrite). The non-linear diffusion terms for microbial movement depend on the concentration of the corresponding limiting nutrient, the concentration of the focal population, the concentration of the other population, and a term for local anisotropy of the biofilm. The rationales for these terms are the following: The dependence on the limiting nutrient ensures that cells only move at the growing edge of the colony, where substrate is available (Mimura *et al*., 2000). Each population is slowed down by the presence of the other population and moves faster when the density of the own population is high (*i.e*. they can push harder together) (Kawasaki *et al*., 1997). This form was chosen to reflect our experimental findings suggesting that spatial constraints and mechanical shoving are the main drivers of dendrite formation of the secondary wave. The anisotropy term represents the local alignment of packs of cells in bacterial biofilms (Volfson *et al*., 2008), but anisotropy can be found in other systems as well (Nittmann and Stanley, 1986).

The model could qualitatively reproduce the dynamics of the two expansions and the formation of dendrites as was observed experimentally. The two populations underwent successive range expansion and the secondary expansion of the consumer formed dendrites with a fractal dimension of 1.798 (SD=0.002) (Figure 4b). If two complete consumers were inoculated together, they rapidly formed sectors as observed experimentally (Figure 4a).

Note that our goal was not to exactly reproduce the patterns found in the experiments, but rather to develop a model that enabled studying how mutations establish in non-dendritic primary or dendritic secondary expansions. In fact, we found that the shape of the dendrites is largely dependent on the anisotropy term, which thus potentially allows us to tune the dendritic structure of the secondary expansion to represent other systems that undergo successive range expansion.

We introduced mutations into our mathematical model to compare the possible evolutionary differences between non-dendritic primary and dendritic secondary expansions. At every time-step the entire population of an active lattice site (i.e. that had substrate available for growth) could mutate with a certain probability from the ancestral population to a new mutant population. The new population then could grow and expand as the ancestral population. We introduced mutations in both the non-dendritic primary and the dendritic secondary expansions. We found that mutant populations rapidly went extinct if the growth rates were exactly the same as the ancestral population.

We thus introduced higher maximal growth rates for the mutants. As the maximal growth rate increased, we found that small patches of mutants first emerged and, if the maximal growth rate was sufficiently higher than the ancestral, the patches could increase in size. The mutants in the non-dendritic primary expansion typically formed patches (Figure 4c) that did not persist for prolonged periods of time unless they had a 50% higher maximal growth rate than the ancestor, at which they rapidly displaced the ancestral population. The mutants in the dendritic secondary expansion, however, could establish dendrites (Figure 4d) that did not disappear throughout the simulations already at 20% higher maximal growth rates. On

348 the other hand it was more difficult for mutants within dendrites to displace the whole
349 resident population because narrow dendrites of the ancestral population could survive,
350 even when they had a large growth disadvantage (see also Supplementary Figure 1).
351
352 To quantify the difference between dendritic and non-dendritic expansion, we measured the
353 fraction of mutants in the actively growing populations at the end of the simulations for
354 different maximal growth rates. The abovementioned dynamics are reflected in the shape of
355 the Gompertz curves that were fitted to the model data (Figure 4e): the lag-parameter
356 (indicated as vertical lines) and the maximum slope of the dendritic secondary population
357 were significantly lower for the non-dendritic primary population than for the dendritic
358 secondary population (F-test, both $p<2.2e-16$), while the maximum proportion was not (F-
359 test, $p=0.379$). This had the consequence that at the point where the proportion of the
360 mutant in the non-dendritic primary expansion started to increase substantially (*i.e.* at the
361 end of the "lag-phase" and with a growth advantage of about 40% compared to the
362 ancestor), the proportion of the mutants in the dendritic secondary expansion already
363 accounted for about half of the active population. This thus supported our hypothesis that
364 mutants establish more readily in the dendritic secondary expansion than in the non-
365 dendritic primary expansion.
366
367 **Discussion**
368 We found that, opposite to our initial expectations (Figure 1), successive range expansion
369 increases intermixing rather than decreases intermixing. The cause for this increase in
370 intermixing is the formation of dendritic patters by the secondary expansion. The branching
371 of the secondary expansion thus creates new local population diversity. In our case, this

372 resulted in higher intermixing than was even observed in the inoculation zone. Increased
373 intermixing signifies higher spatial heterogeneity, shorter average distances between the
374 two populations and increased interface size. This could affect how the two populations
375 interact with each other, e.g. by exchange of goods such as metabolites (Kolenbrander *et al*.,
376 2010), and it could facilitate genetic exchange, e.g. the probability of horizontal gene
377 transfer is proportional to the number of cell-cell contacts (Sørensen *et al*., 2005; Niehus *et*
378 *al*., 2015).
379
380 Over longer time-scales, more genetic diversity might establish in the dendritic secondary
381 expansion than in the non-dendritic primary expansion. Our modeling results show that
382 mutations with small growth advantages establish more readily during dendritic expansion.
383 Because mutations that confer small fitness advantages are likely more common than
384 mutations that confer large fitness advantages (Elena and Lenski, 2003), we expect that
385 more mutations will accumulate in the secondary dendritic expansion. The branching of the
386 secondary dendritic expansion can therefore mitigate the loss of diversity due to two
387 mechanisms: increased intermixing between the secondary and primary populations and
388 higher accumulation of novel mutations in the secondary population during extended
389 periods of expansion.
390
391 The main driver of the branching process is the reduced availability of resources to the
392 secondary population, which must expand into areas already colonized by the primary
393 population. Here we identified space as an important limiting resource when expanding into
394 a previously colonized area. The importance of spatial constraints for branching of the
395 secondary expansion suggests that branching could be a general process that potentially

affects many populations with limited dispersal capabilities. One example could be tumors that penetrate into the surrounding tissue (Anderson and Quaranta, 2008), where the healthy tissue represents the already colonized area (*i.e*., the primary expansion) and the tumor represents the secondary expansion. Since tumors have high mutation rates and form dendritic patters, the accumulation of mutations may play an important role in this case. Another example are plants, which usually grow in clustered groups (Dale, 1999). A secondary expansion could thus resemble percolation clusters, which also consist of many small localized regions and exhibit fractal properties. Finally, these processes could potentially also be important for our own species. A recent analysis of the Native American population structure suggests that there were three successive immigration events into the Americas and that there was extensive admixture between the first and the following populations (Reich *et al*., 2012). In all of these cases, the branched pattern of the secondary expansion does not have to be exactly the same that we observed in this study. The important point is that secondary expansion leads to splitting of the expansion front into small local sub-populations, which increases intermixing with the primary expansion and may lead to increased accumulation of mutations in the secondary expansion.

Conflict of interest

The authors declare no conflict of interest.

References

1. Anderson AR, Quaranta V. (2008). Integrative mathematical oncology. *Nat Rev Cancer* **8**: 227–234.
2. Ben-Jacob E, Schochet O, Tenenbaum A, Cohen I, Czirók A, Vicsek T. (1994). Generic

420 modelling of cooperative growth patterns in bacterial colonies. *Nature* **368**: 46–49.
421 3. Cavalli-Sforza LL, Menozzi P, Piazza A. (1993). Demic expansions and human evolution.
422 *Science* **259**: 639–646.
423 4. Connell JH, Slatyer RO. (1977). Mechanisms of succession in natural communities and
424 their role in community stability and organization. *Am Nat* **111**: 1119-1144.
425 5. Dale MRT. (1999). *Spatial Pattern Analysis in Plant Ecology*. Cambridge University Press:
426 Cambridge, United Kingdom.
427 6. Elena SF, Lenski RE. (2003). Evolution experiments with microorganisms: the dynamics
428 and genetic bases of adaptation. *Nat Rev Genet* **4**: 457–469.
429 7. Excoffier L, Foll M, Petit RJ. (2009). Genetic consequences of range expansions. *Annu Rev*
430 *Ecol Evol Syst* **40**: 481–501.
431 8. Excoffier L, Ray N. (2008). Surfing during population expansions promotes genetic
432 revolutions and structuration. *Trends Ecol Evol* **23**: 347–351.
433 9. Fujikawa H, Matsushita M. (1989). Fractal growth of *Bacillus subtilis* on agar plates. *J*
434 *Phys Soc Japan* **58**: 3875–3878.
435 10. Golding I, Kozlovsky Y, Cohen I, Ben-Jacob E. (1998). Studies of bacterial branching
436 growth using reaction–diffusion models for colonial development. *Physica A* **260**: 510–
437 554.
438 11. Hallatschek O, Hersen P, Ramanathan S, Nelson DR. (2007). Genetic drift at expanding
439 frontiers promotes gene segregation. *Proc Natl Acad Sci U S A* **104**: 19926–19930.
440 12. Hewitt G. (2000). The genetic legacy of the Quaternary ice ages. *Nature* **405**: 907–913.
441 13. Kawasaki K, Mochizuki A, Matsushita M, Umeda T, Shigesada N. (1997). Modeling spatio-
442 temporal patterns generated by Bacillus subtilis. *J Theor Biol* **188**: 177–185.
443 14. Kolenbrander PE, Palmer RJ, Periasamy S, Jakubovics NS. (2010). Oral multispecies

biofilm development and the key role of cell-cell distance. *Nat Rev Microbiol* **8**: 471–480.

15. Lalucat J, Bennasar A, Bosch R, García-Valdés E, Palleroni NJ. (2006). Biology of Pseudomonas stutzeri. *Microbiol Mol Biol Rev* **70**: 510–547.
16. Lilja EE, Johnson DR. (2016). Segregating metabolic processes into different microbial cells accelerates the consumption of inhibitory substrates. *ISME J* **10**: 1568-1578.
17. Mather W, Mondragón-Palomino O, Danino T, Hasty J, Tsimring LS. (2010). Streaming Instability in Growing Cell Populations. *Phys Rev Lett* **104**: 208101.
18. Mathiesen J, Procaccia I, Swinney HL, Thrasher M. (2006). The universality class of diffusion-limited aggregation and viscous fingering. *Europhys Lett* **76**: 257–263.
19. May SE, Maher J V. (1989). Fractal dimension of radial fingering patterns. *Phys Rev A* **40**: 1723–1726.
20. Mimura M, Sakaguchi H, Matsushita M. (2000). Reaction – diffusion modelling of bacterial colony patterns. *Physica A* **282**:283–303.
21. Momeni B, Brileya KA, Fields MW, Shou W. (2013). Strong inter-population cooperation leads to partner intermixing in microbial communities. *Elife* **2**:e00230.
22. Niehus R, Mitri S, Fletcher AG, Foster KR. (2015). Migration and horizontal gene transfer divide microbial genomes into multiple niches. *Nat Commun* **6**: 8924.
23. Nittmann J, Stanley HE. (1986). Tip splitting without interfacial tension and dendritic growth patterns arising from molecular anisotropy. *Nature* **321**: 663–668.
24. Pielou EC. (1966). Species-diversity and pattern-diversity in the study of ecological succession. *J Theor Biol* **10**: 370–383.
25. Reich D, Patterson N, Campbell D, Tandon A, Mazieres S, Ray N, *et al*. (2012). Reconstructing Native American population history. *Nature* **488**: 370–374.
26. Rickard AH, Gilbert P, High NJ, Kolenbrander PE, Handley PS. (2003). Bacterial

coaggregation: an integral process in the development of multi-species biofilms. *Trends Microbiol* **11**: 94–100.

27. Sokal RR, Oden NL, Wilson C. (1991). Genetic evidence for the spread of agriculture in Europe by demic diffusion. *Nature* **351**: 143–145.

28. Sørensen SJ, Bailey M, Hansen LH, Kroer N, Wuertz S. (2005). Studying plasmid horizontal transfer in situ: a critical review. *Nat Rev Microbiol* **3**: 700–710.

29. Tilman D, Kareiva PM. (1997). *Spatial Ecology: The Role of Space in Population Dynamics and Interspecific Interactions*. Princeton University Press: Princeton, NJ.

30. van de Koppel J, Gupta R, Vuik C. (2011). Scaling-up spatially-explicit ecological models using graphics processors. *Ecol Modell* **222**: 3011–3019.

31. Volfson D, Cookson S, Hasty J, Tsimring LS. (2008). Biomechanical ordering of dense cell populations. *Proc Natl Acad Sci U S A* **105**: 15346–15351.

32. Zumft WG. (1997). Cell biology and molecular basis of denitrification. *Microbiol Mol Biol Rev* **61**: 533–616.

Acknowledgments

We thank Fordyce A. Davidson for valuable insights and suggestions on how to design the non-linear diffusion term of the microbial populations in the model; Lara Pfister, Selina Derksen-Müller, and Anja Bernet for help with the strain construction; Lea Caduff for help with the microscopy; and Martin Ackermann and Will Macnair for helpful discussions and comments on early versions of the manuscript. This work was supported by grants from the Swiss National Science Foundation (31003A_149304) and SystemsX.ch, The Swiss Initiative in Systems Biology (MicroScapesX.ch).

492 Supplementary Information accompanies the paper on The ISME Journal website
493 (http://www.nature.com/ismej)
494
495 **Figure Legends**
496
497 **Figure 1. Schematic illustration of (a) simultaneous and (b) successive range expansion**
498 **(quarter circles of radial expansions).** In panel **a,** the green and blue colored areas represent
499 two populations that have the same growth properties. In the inoculation zone (lower left)
500 the two populations are well mixed. During expansion, genetic drift at the expansion front
501 causes the two populations to segregate into sectors, which reduces intermixing and local
502 population diversity. The boundaries are parallel to the direction of expansion because the
503 growth properties of the two populations are identical. Panel **b** represents a successive
504 range expansion of a primary population (blue) and a secondary population (green). The
505 successive expansion could cause a segregation of the primary from the secondary
506 population perpendicular to the direction of expansion, which would lead to two successive
507 waves and an even further reduction in intermixing and local population diversity.
508
509 **Figure 2. Expansion of co-cultures of complete degraders or co-cultures of the producer**
510 **and consumer and quantification of intermixing. A1+2)** For co-cultures of complete
511 degraders, sectors with boundaries lying parallel to the axis of expansion emerged. **B1+2)**
512 For co-cultures of producers and consumers, two successive expansions emerged, where the
513 producer (blue) formed a continuous non-dendritic expansion while the consumer (green)
514 formed a dendritic expansion**. C)** Measurement of intermixing between the producer and
515 the consumer from the center of colonies towards the edge of expansion **Left)** Intermixing

index at radial position, the blue line is a loess smoother, the red lines indicate the beginning and end of the secondary expansion by the consumer (see the Supplementary Information). Intermixing is relatively constant in the inoculum, then increases and peaks in the expansion zone. **Right)** Intermixing in the secondary expansion is significantly higher than in the inoculum (Mann-Whitney test, $p < 2.2e-16$).

Figure 3. Microscopy images of range expansions with different growth limiting factors that were devised to assess the causes of dendrite formation. A1+2) Co-cultures of the producer (blue) and consumer (red) grown together with exogenous supplies of both nitrate and nitrite. The area outside of the colony was colored white to visualize the expansion edge (A2 magnification). The strains still succeeded each other and the consumer formed dendrites even though nitrite was added exogenously. **B)** Co-cultures of the consumer grown alone (in green and red) on plates containing nitrite, which did not form dendrites. **C)** The producer (blue) expanding into space previously occupied by the consumer (green) on plates containing exogenous supplies of both nitrate and nitrite, where the producer formed dendrites.

Figure 4. Modeling results and predictions. A) Two completely degrading populations rapidly segregated into sectors. **B)** The secondary expansion of the consumer produced fractal dendrites (Magnifications of sections of the modeled circular colonies are shown). In the second row the model output with mutants that have a 1.4 times higher maximum growth rate than the ancestor. Blue is the primary and green the secondary population. In panel **C,** the red areas indicate mutants in the primary population. It can be seen that they form patches that go extinct relatively rapidly. In panel **D,** the mutants (also red) are

introduced in the secondary population. In contrast to the mutants in the primary population in panel C, they can take over dendrites and establish locally. **E)** Measurement of the proportion of the mutant in the actively growing part of the population at the end of a simulation at different relative growth advantages. Blue is the non-dendritic primary expansion of the producer, green is the dendritic secondary expansion of the consumer. The data points represent independent simulations. The curves show the Gompertz-model fits and the vertical lines represent the lag-parameter of these models with 95% confidence intervals in grey.

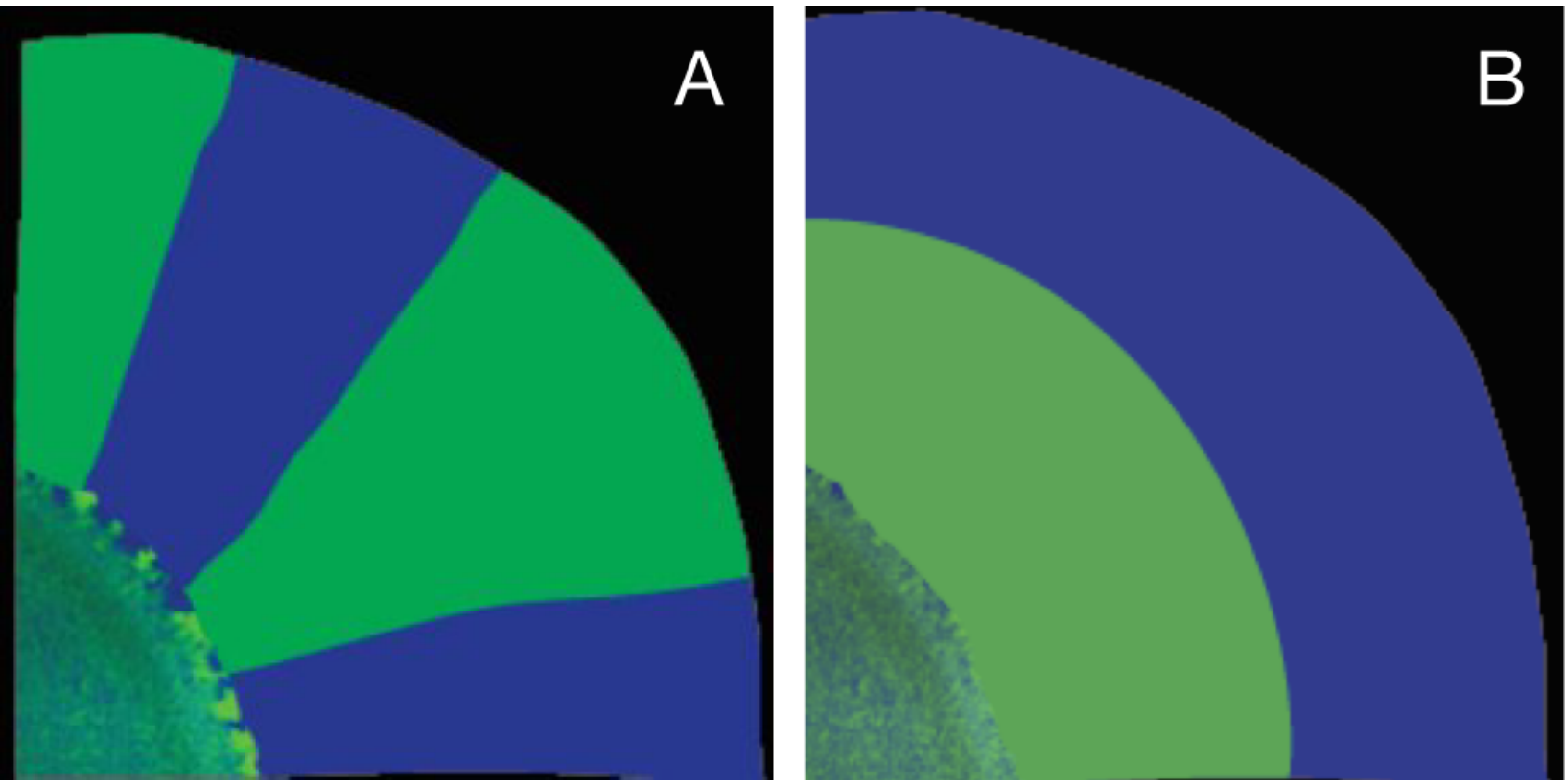
A
B

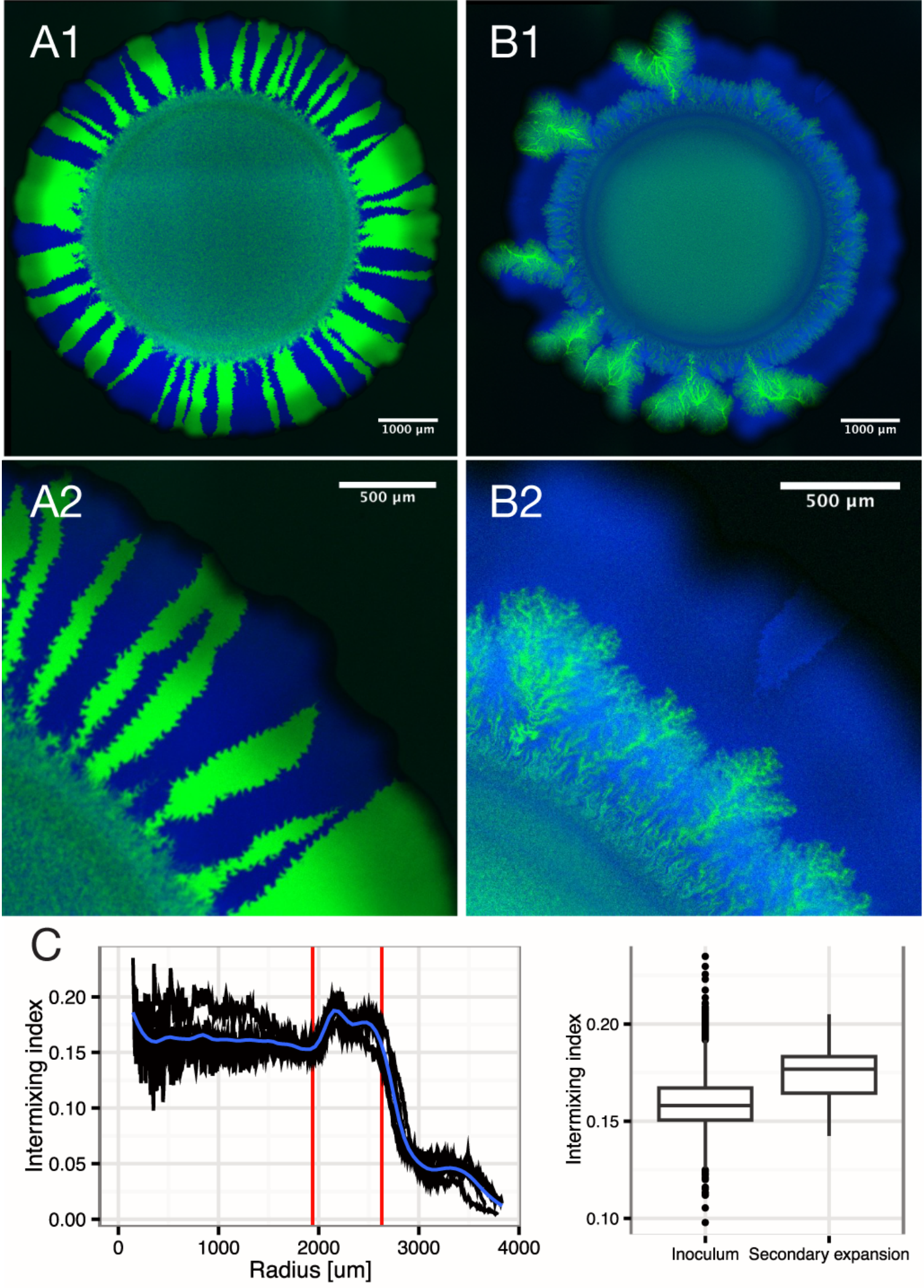
A1
1000 µm
B1
1000 µm
A2
500 µm
B2
500 µm
C
Intermixing index
0.20
0.15
0.10
0.05
0.00
0
1000
2000
3000
4000
Radius [um]
Intermixing index
0.20
0.15
0.10
Inoculum
Secondary expansion

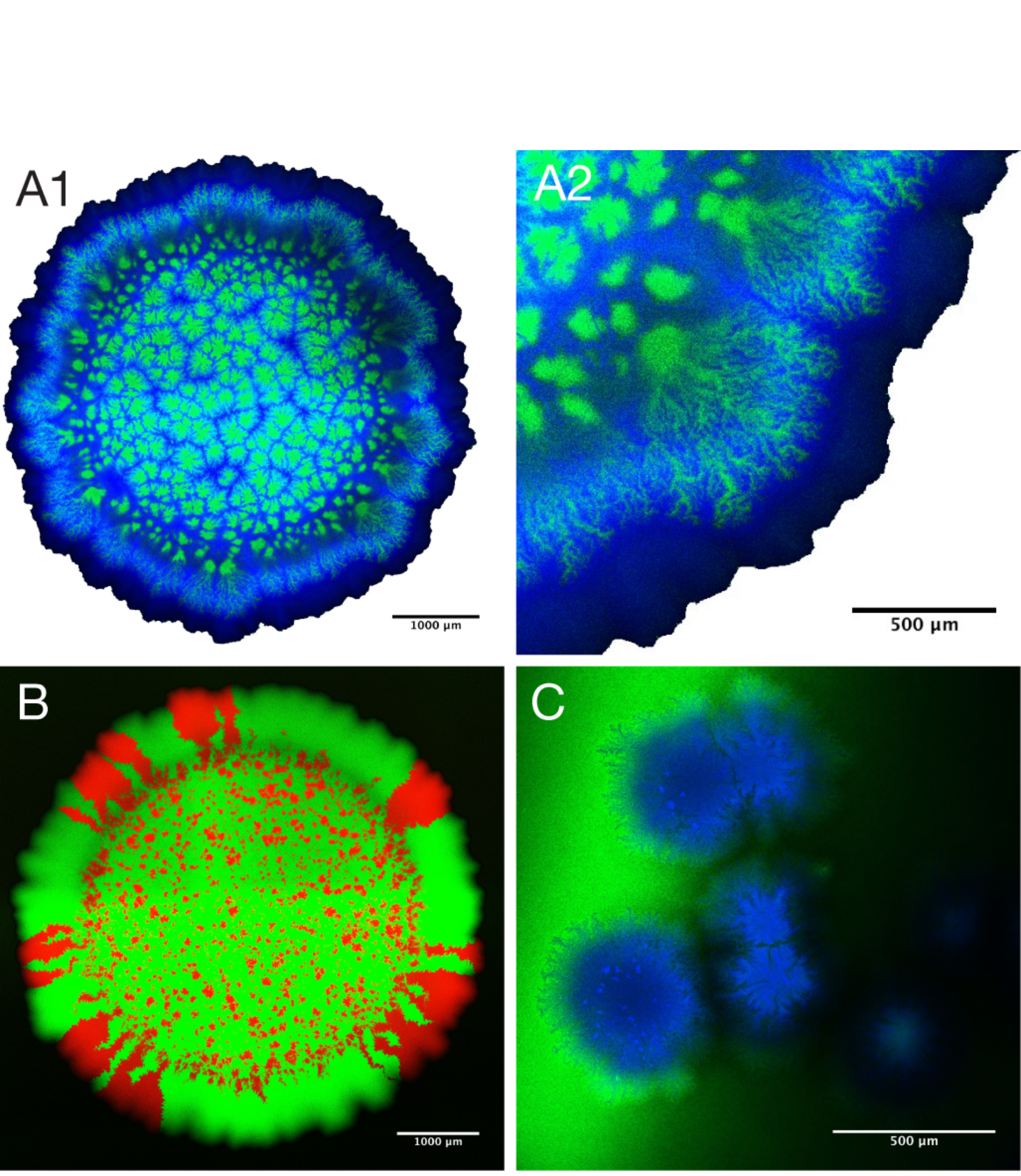
A1
1000 µm
A2
500 µm
B
1000 µm
C
500 µm

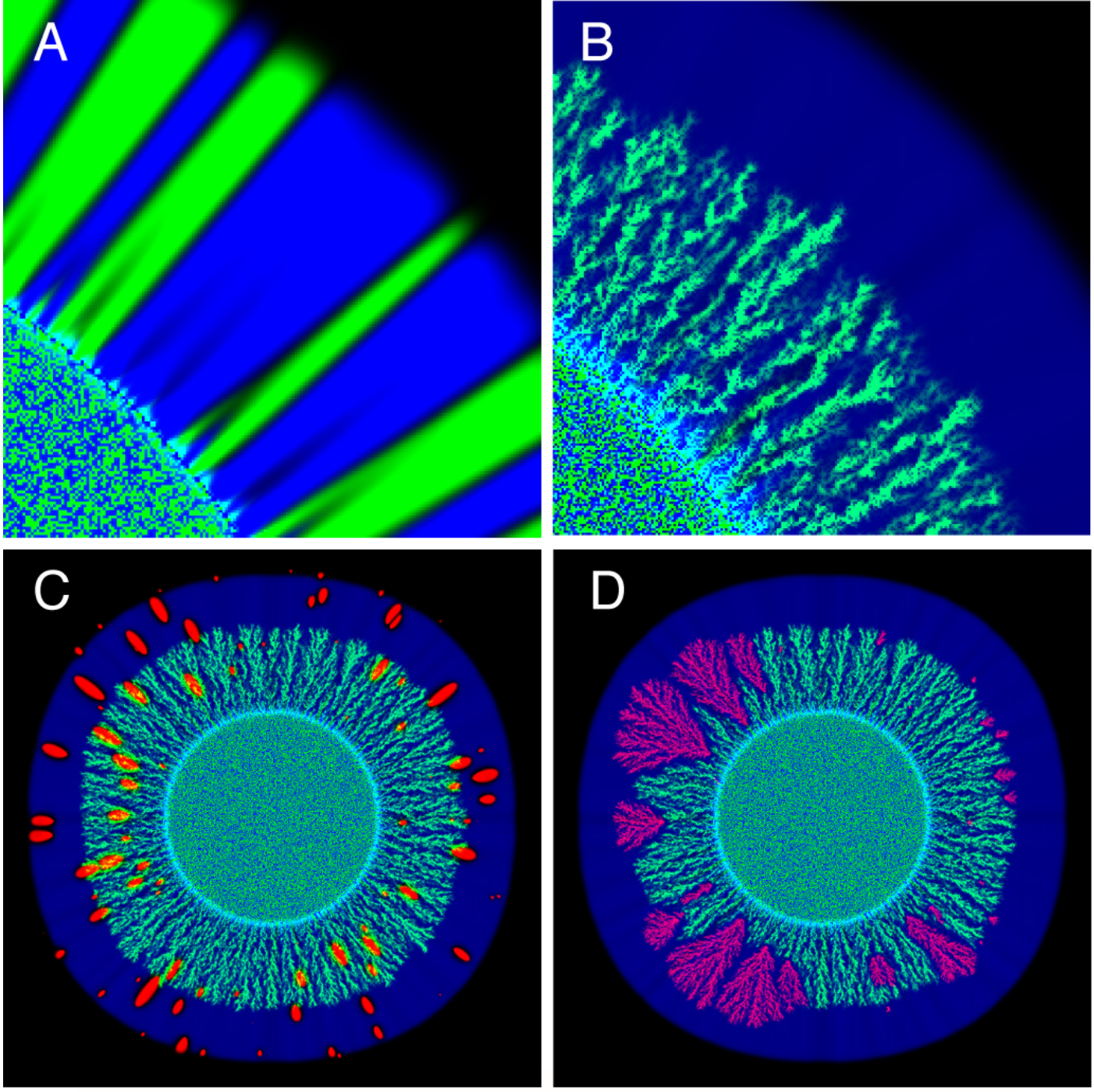
A
B
C
D

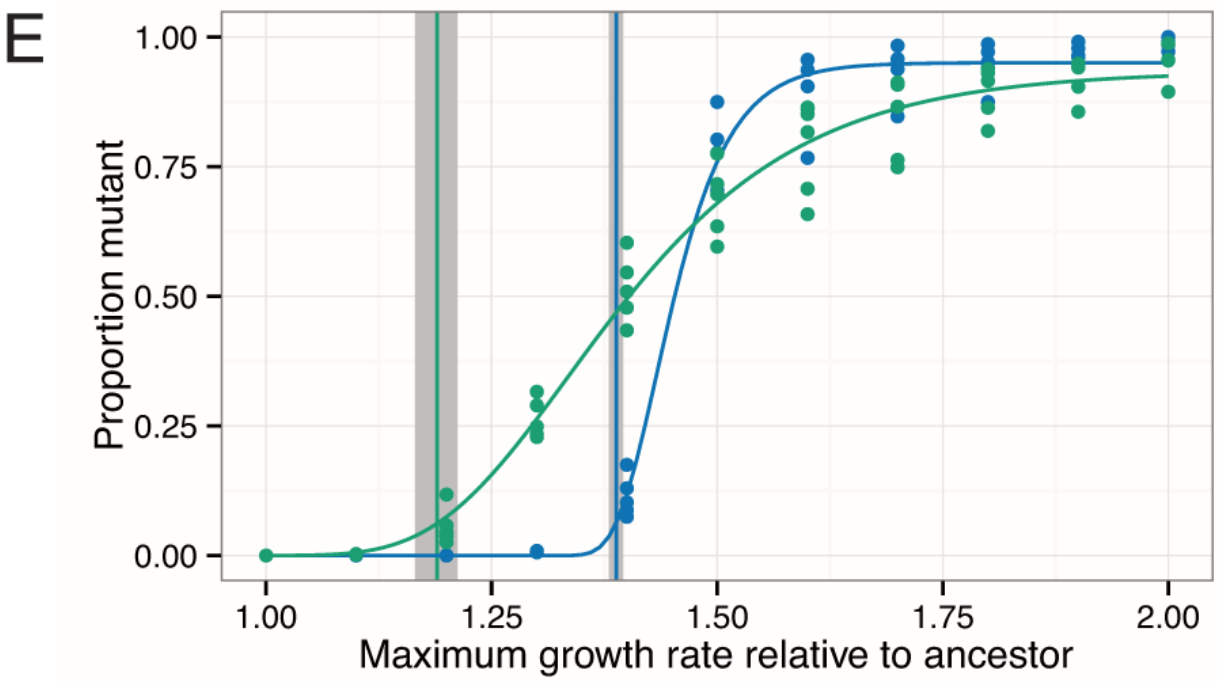
E
1.00
0.75
0.50
0.25
0.00
Proportion mutant
1.00
1.25
1.50
1.75
2.00
Maximum growth rate relative to ancestor